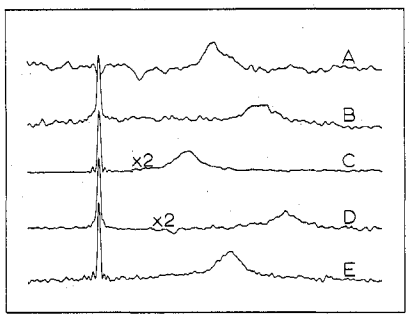

Figure 1. ^{14}N NMR spectra at 4.3 MHz obtained by Fourier transform. Full-scale sweep width on all spectra is 4108 Hz with frequency increasing to the right. The low-frequency nitrate signals in spectra B–E are incompletely apodized. The sample temperature was 30 ± 1 °C: A, spectrum of 1.25 M hexanitrocobaltate(III) ion freshly dissolved (20 000 transients); B, spectrum of solution A after standing for 2 h (10 000 transients); C, spectrum of 1 M $NaNO_3$ and 5 M $NaNO_2$ (5000 transients); D, spectrum of 1.25 M hexanitrocobaltate(III) ion which is 5.4 mM in Co^{2+} by addition of aqueous cobalt chloride (20 000 transients); E, spectrum of 1.25 M hexanitrocobaltate(III) ion which is 1.9 M in sodium nitrite (20 000 transients).

complex which is labile and catalyzes exchange of the free ligand with the cobalt(III) complex and also causes a large paramagnetic shift.

It is important to note that addition of the same amount of cobalt(II) ion that was used in obtaining the spectrum of Figure 1D to a solution of nitrate and nitrite ions does not cause an observable shift in the ^{14}N spectrum of either anion. Since the ^{14}N spectra of Figure 1B,D,E show an exchange-averaged nitrite ion line, the cobalt(II) ion apparently catalyzes rapid exchange of ligand with the cobalt(III) complex. It is likely that the catalysis involves an electron transfer.

These chemical complications make estimation of the cobalt–nitrogen coupling constant more uncertain because even extrapolation to zero time does not guarantee that the ^{14}N line width in the hexanitrocobaltate ion will accurately reflect T_1 because of the possible exchange contributions. With this caution, the necessary relaxation data are summarized in Table I for solutions of the complex in water and deuterium oxide. The changes in the cobalt T_1 and the nitrogen line width reflect the differences in the viscosity of the two solvents in the usual way. It is clear, however, that the cobalt line width has the inverted dependence on solution viscosity expected for a dominant contribution from scalar relaxation of the second kind. Coupling constants from both sets of data were used independently to calculate J_{Co-N}. Both calculations give the value of 46 ± 4 Hz. This result is 20% smaller than that obtained in the same way for hexaamminecobalt(III) ion.[3]

In view of these results, it appears that the conclusions drawn about the nitrogen spectra in the nitro complexes of platinum and palladium[8] need to be reexamined and it appears that scalar relaxation mechanisms need to be considered very carefully when the metal resonances are investigated in nitrogen coordinated systems.

Acknowledgment. This work was supported by the Dreyfus Foundation, the National Institutes of Health (Grants GM18719 and GM21335), and the Chemistry Department, University of Minnesota.

Registry No. $Co(NO_2)_6^{3-}$, 15079-20-6.

References and Notes

(1) Camille and Henry Dreyfus Teacher-Scholar.
(2) (a) F. Yajima, Y. Koike, A. Yamasaki, and S. Fujiwara, *Bull. Chem. Soc. Jpn.*, **47**, 1442 (1974); (b) T. Raj and R. G. Bryant, *J. Magn. Reson.*, in press.
(3) K. D. Rose and R. G. Bryant, unpublished data.
(4) G. Brauer, "Handbuch der Präparativen Anorganischen Chemie", Ferdinand Euke Verlag, Stuttgart, 1954, p 1151.
(5) R. Ader and A. Loewenstein, *J. Magn. Res.*, **5**, 248 (1971).
(6) A. Abragam, "Principles of Nuclear Magnetism", Clarendon Press, Oxford, 1961, p 313.
(7) Reference 6, p 309.
(8) R. Bramley, B. N. Figgis, and R. S. Nyholm, *J. Chem. Soc. A*, 861 (1967).
(9) J. B. Willis, J. A. Friend, and D. P. Mellor, *J. Am. Chem. Soc.*, **67**, 1680 (1945).

Contribution from the Departments of Chemistry, Northwestern University, Evanston, Illinois 60201, and Massachusetts Institute of Technology, Cambridge, Massachusetts 02139

Spectroscopic and Theoretical Analysis of the Intense $^1T_{1u} \leftarrow {}^1A_{1g}$ Transitions in $Mo(CO)_6$ and $W(CO)_6$

WILLIAM C. TROGLER,*[1a] SYLVIE R. DESJARDINS,[1b] and EDWARD I. SOLOMON*[1b]

Received January 19, 1979

Optical spectra of $M(CO)_6$ (M = Mo, W) complexes have been measured in argon matrices at 10 K, focusing on the intense $^1T_{1u} \leftarrow {}^1A_{1g}$ transitions at 286 and 230 nm. Vibrational structure is observed on the 286-nm band. A detailed band shape analysis is performed on both absorption bands, and accurate excited-state electronic parameters are obtained. The distortion of the CO moiety is found to be small for both transitions, particularly for the 286-nm one. Transition-state Xα calculations have been performed for the low-lying allowed metal to ligand and ligand to metal charge-transfer transitions as well as for the metal-localized $d(t_{2g}) \rightarrow p(t_{1u})$ excitation. The results confirm assignment of the electronic absorption bands to $d(t_{2g}) \rightarrow CO(\pi^*)(t_{1u}$ and $t_{2u})$; however, the π^* levels of CO in the metal hexacarbonyls prove to differ considerably from the π^* level in free CO. Relative amounts of charge reorganization calculated for the excited states provide a rationale of the spectroscopically derived parameters.

Both extended Hückel[2] and more elaborate calculations[3] provide a basis for understanding many aspects of the electronic structure of metal hexacarbonyl complexes. At this point satisfactory agreement between photoelectron spectra and calculated ionization potentials has been realized for $Cr(CO)_6$.[2,3] Additionally, reasonable assignments of the low-resolution electronic absorption spectra of $M(CO)_6$ (M = Cr, Mo, W) have been proposed on the basis of molecular orbital calculations combined with the spectroscopic effects of chemical variation.[2] These studies assign the low-energy tail in the electronic absorption spectra of the metal hexacarbonyls as ligand field transitions. In addition, two intense spectral features (found at ca. 286 and 230 nm) are assigned as allowed $^1T_{1u} \leftarrow {}^1A_{1g}$ transitions arising from one-electron excitation processes which originate in the metal $t_{2g}(d)$ orbitals and terminate in the t_{1u} and t_{2u} ligand π^* orbitals (i.e., M $d(t_{2g}) \rightarrow CO(\pi^*)$).[2-4] A detailed assignment of the electronic absorption spectra and a determination of the nature of the

0020-1669/79/1318-2131$01.00/0

associated excited states is of obvious importance based on their role in photochemical processes.[4]

Upon cooling to 10 K, $Mo(CO)_6$ and $W(CO)_6$ (but not $Cr(CO)_6$) in Ar–CO_2 matrices exhibit a reasonable amount of vibrational structure on their electronic absorption bands and permit a detailed spectral analysis. The vibronic band shapes are interpreted in terms of excited-state distortions via a Franck–Condon analysis and, then, correlated with results of a first-principles quantum mechanical calculation on $Mo(CO)_6$ (as previous calculations have been limited to $Cr(CO)_6$). The combined spectroscopic and theoretical data present a precise picture of bonding in "charge-transfer" excited states of the metal hexacarbonyls.

Experimental Section

Optical spectra were obtained with a Cary 17D spectrophotometer, whose sample compartment was cut away to permit access of the matrix-isolation equipment. The latter apparatus consists of a Displex CS 202B refrigeration unit modified for pulsed-deposition matrix isolation[5] and equipped with CaF_2 windows. Matrices were deposited on a sapphire window carefully affixed in the cold-station ring mount with indium gaskets. Failure to ensure good thermal contact between the window and cold station yields poor optical matrices. A base pressure of less than 10^{-6} torr was observed prior to deposition. Generally 2–25 pulses (10 mL volume at 50–500 torr) of the metal hexacarbonyl at greater than 1000-fold dilution in Ar, 2:1 Ar–CO_2 and 3:1 Ar–CO_2, were applied. Matrix thickness was nearly linear with the number of pulses under these conditions (judged by complex absorbance). Argon (99.9998%) and carbon dioxide (99.999%) were obtained from Airco and used without further purification. Metal hexacarbonyls were recrystallized from toluene and sublimed three times prior to use. Independent observation of the matrix infrared spectra (1600–2100 cm^{-1}) with a Nicolet 7199 FT IR agreed with literature spectra[6] for $M(CO)_6$ (M = Cr, Mo, W) complexes in argon matrices. A sample temperature of nominally 10 K was measured with a calibrated Fe-doped Au thermocouple affixed to the cold station.

Vibronic band shapes were generated[7,8] by using progressions in one or two normal modes (of different frequencies) built upon a Gaussian origin of the form

$$g(\nu) = \left(\frac{4 \ln 2}{\pi}\right)^{1/2} \frac{1}{b} \exp\left[-4 \ln 2 \left(\frac{\nu - c}{b}\right)^2\right] \qquad (1)$$

where b is the full width at half-maximum, and c is the frequency corresponding to the maximum of the Gaussian. The band shapes generated by harmonic vibrational progressions in two modes (1 and 2) are determined at $T \simeq 0$ K by

$$I(\nu) = e^{-(S_1+S_2)} \sum_{n_1} \sum_{n_2} g(\nu - n_1\nu_1 - n_2\nu_2) \frac{S_1^{n_1} S_2^{n_2}}{n_1!\, n_2!} \qquad (2)$$

where $n_{1,2}$ and $\nu_{1,2}$ ($= k_{1,2}^{1/2}/2\pi\mu_{1,2}^{1/2}$) are the vibrational quanta and frequencies, and $S_{1,2}$ are the Franck–Condon factors. Theoretical band shapes were fit to corrected experimental spectra employing a steepest-descent method within a least-squares fitting program.

Hartree–Fock–Slater calculations were performed on a CDC 6600 computer using the discrete variational method[9] (DVM) and iterating to self-consistent charge. Only the s-wave part of the potential was used for computing Coulomb integrals.[9] The Xα exchange parameter was fixed at 0.70 for all calculations. Basis functions were numerical atomic orbitals (NAO's) generated by atomic HFS calculations. Separate spin-restricted "transition-state"[10] calculations predicted the energy for each electronic transition. Atomic basis orbital populations were computed as follows. The atomic orbital charge density contribution to the jth eigenvector in a given symmetry block is

$$Q_j = q_{jj} + \sum_{k \neq j} \left(\frac{q_{jj}}{q_{jj} + q_{kk}}\right) q_{jk} \qquad (3)$$

where q_{jj} is the diagonal density and the second term weights the distribution of the "bond densities" q_{jk}. Experimental bond distances and angles for $Mo(CO)_6$[11] and free CO[12] were used in the calculations.

Results and Discussion

A. Spectral Methods. When the optical spectra of $M(CO)_6$ (M = Cr, Mo, W) complexes were measured in argon matrices at 10 K, $Mo(CO)_6$ and $W(CO)_6$ exhibited vibrational structure on the 286-nm (35 000-cm^{-1}) electronic absorption band (Figure 1). The vibronic structure is independent of the $M(CO)_6$ concentration, the matrix thickness, the sample purification procedure, and the gas composition (Ar–CO_2 mixtures). This band has been assigned[2,3] to the allowed charge-transfer excitation $^1T_{1u} \leftarrow {}^1A_{1g}$ ($d(t_{2g}) \rightarrow CO(\pi^*)(t_{1u})$). The oscillator strength of ca. 0.1 clearly demonstrates that the transition is electric-dipole-allowed.[2] In O_h symmetry this requires a $^1T_{1u} \leftarrow {}^1A_{1g}$ assignment. Hereafter we restrict

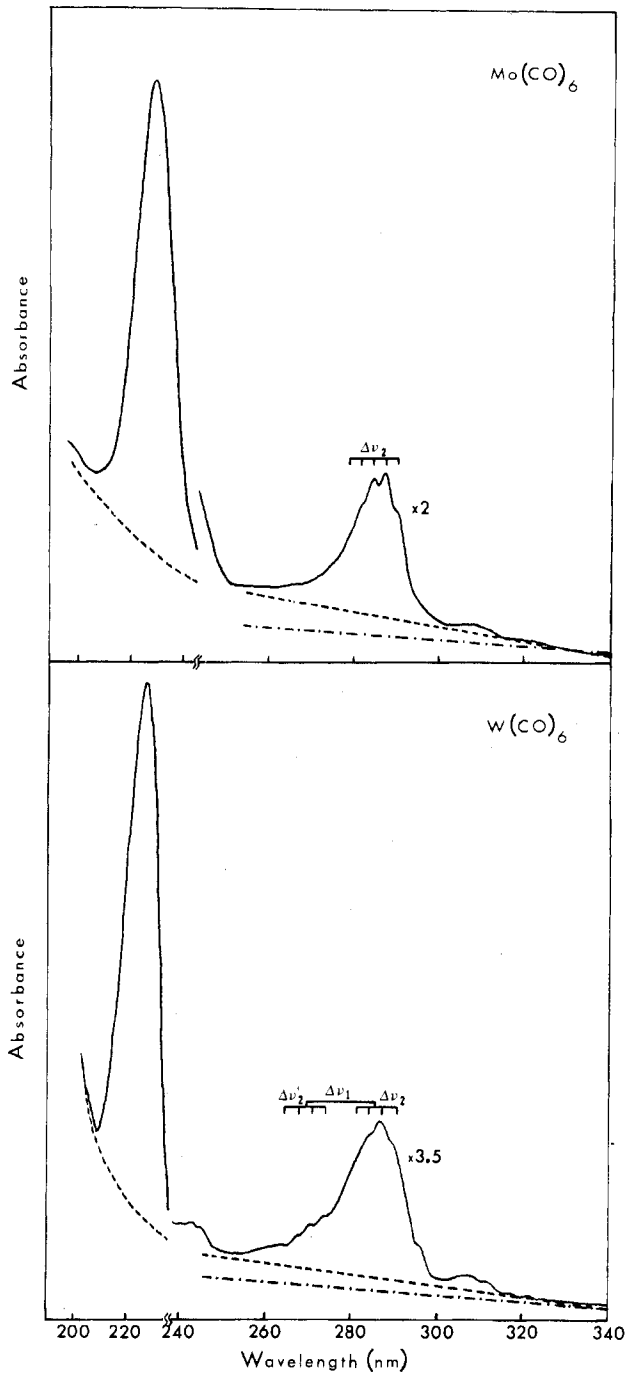

Figure 1. Electronic absorption spectra of $Mo(CO)_6$ and $W(CO)_6$ (greater than 1000-fold dilute) in an argon matrix at 10 K. The two different backgrounds which have been subtracted for the Franck–Condon analysis are as follows: –·–, background A; ---, background B. The matrix was deposited onto a cooled sapphire substrate by employing the pulsed technique. The multiplying factor on the low-energy band was obtained from the number of pulses applied in each region (see Experimental Section). Spectra were measured by maintaining a spectral bandwidth less than 0.1 nm.

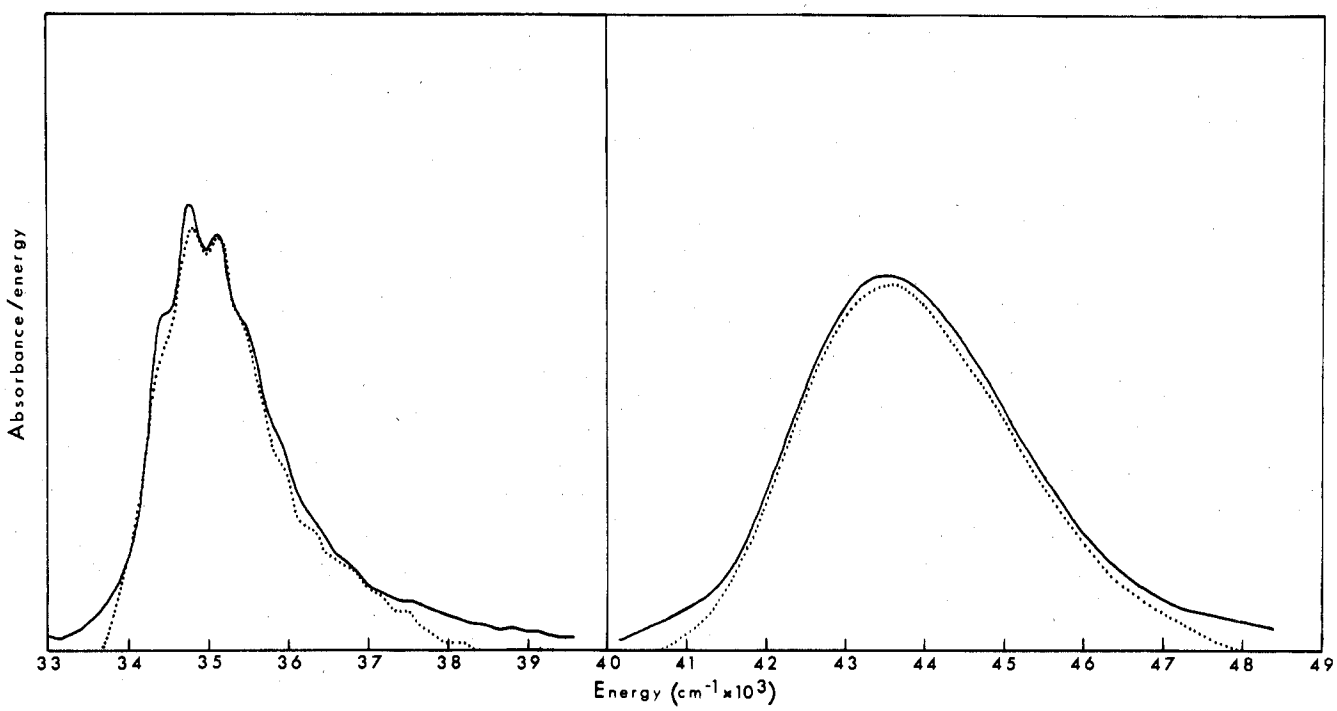

Figure 2. Comparison of the corrected experimental (full line) and generated (dotted line, reduced by a factor of 0.97 for clarity) band shapes for the intense $^1T_{1u} \leftarrow {}^1A_{1g}$ transitions in $Mo(CO)_6$.

consideration to one-electron excitations which result in $^1T_{1u}$ electronic states. In the absence of large excited-state Jahn–Teller distortions, the vibrational progressions observed in absorption must be attributed to excited-state a_{1g} fundamentals.[8,13] There are two a_{1g} normal modes of vibration in a $M(CO)_6$ molecule. For both ground-state $Mo(CO)_6$ and $W(CO)_6$ ν_1, which is predominantly a C–O stretching vibration of a_{1g} symmetry, occurs at 2124 cm^{-1}.[14] The other a_{1g} fundamental, ν_2, consists chiefly of metal–carbon bond stretching and occurs at 392 cm^{-1} for $Mo(CO)_6$ and 420 cm^{-1} for $W(CO)_6$.[14] Cognizant of this background information the spectra in Figure 1 will be analyzed.

The 286-nm absorption in $Mo(CO)_6$ exhibits only one major progression in a 350-cm^{-1} vibration ($\Delta\nu_2$ in Figure 1). We attribute this to the ν_2 vibration in the excited state. A progression in the high-frequency ν_1 mode is not evident. The spectral features displayed by $W(CO)_6$ are similar except for a peak at ca. 296–297 nm which is not present in $Mo(CO)_6$. As for $Mo(CO)_6$ an excited-state ν_2 progression (ca. 400 cm^{-1}) is observable ($\Delta\nu_2$ in Figure 1). The peak at ca. 296–297 nm apparently does not follow this progression. The fact that ν_2 in the analogous $W(CO)_6$ excited state is of higher frequency than that in $Mo(CO)_6$ parallels the order of the ground state ν_2's (vide supra). Importantly, a second weak set of low-frequency (400 cm^{-1}) progressions ($\Delta\nu'_2$ in Figure 1) appears to higher energy of the 286-nm band. This we assign to a progression in the other a_{1g} mode, ν_1. A more intense electronic absorption band occurs at ca. 230 nm in both $Mo(CO)_6$ and $W(CO)_6$ (Figure 1); however, no vibronic structure appears on this band. To extract more precise values for the excited-state parameters, we present below a detailed Franck–Condon analysis of the band shapes.

For the first intense UV absorption band, the following parameters are allowed to vary in eq 1 and 2: S_1, S_2, ν_1, ν_2, and c. The structure on this transition is not sufficient to allow an independent fit of b; however, this parameter may be estimated as $\simeq$400 cm^{-1} from a qualitative observation of the "amount" of structure on the absorption band. Lack of structure precludes an independent fit of S_2 and ν_2 for the second UV transition at 230 nm. A best fit, obtained by equating these to zero, does allow for their effect by permitting b to vary. The next logical step of fixing S_1 and ν_1 to the values thus obtained and b to 400 cm^{-1} (as found from the first transition) while S_2 and ν_2 are varied is not satisfactory as it produces a structured band shape. The final results for the two first intense UV bands in $Mo(CO)_6$ and $W(CO)_6$ are listed in Table I, and the calculated and experimental band shapes are compared in Figures 2 and 3.

Table I. Franck–Condon Factors and Excited-State Frequencies and Distortions Obtained from the Least-Squares Fitting Procedure

compd	band, nm	S_1	S_2	ν_1, cm^{-1}	ν_2, cm^{-1}	b, cm^{-1}	ΔQ_1, Å	ΔQ_2, Å
$Mo(CO)_6$	286	0.14	2.9	1950	380	400	0.03	0.16
	230	0.77		1300		2150	0.08	
$W(CO)_6$	286	0.24	2.7	1840	410	400	0.04	0.15
	230	0.74		1190		1500	0.08	

The agreement between the experimental and theoretical overall band shapes in Figures 2 and 3 is quite reasonable on the basis of the results for analogous band shape analysis approaches on other inorganic complexes[8,15] and supports the simplifications used in this treatment. Further, the calculated (Table I) and observed ν_2 progressional spacings on the first absorption band for both complexes are found to be in close agreement [for $Mo(CO)_6$, ν_2(calcd best fit) = 380 cm^{-1} and ν_2(exptl) $\simeq$ 350 cm^{-1}; for $W(CO)_6$, ν_2(calcd best fit) = 410 cm^{-1} and ν_2(exptl) $\simeq$ 400 cm^{-1}]. Similarly, the calculated ν_1 spacings appear to be reasonable [for $Mo(CO)_6$, ν_1(calcd best fit) = 1950 cm^{-1}; for $W(CO)_6$, ν_1(calcd best fit) = 1840 cm^{-1}; for both complexes, ν_1(exptl, ground state) = 2124 cm^{-1} [14]]; these could not be estimated visually directly from the data as this approach would be subject to at least one ν_2 quantum of error. Small disagreements are observed in the relative intensities of some individual vibrational quanta (Figures 2 and 3); however, this is to be expected with a model utilizing only a very limited number of adjustable parameters.

The sensitivity of the parameters obtained by fitting to a somewhat flexible experimental band shape can now be explored to estimate their reliability. We considered the fol-

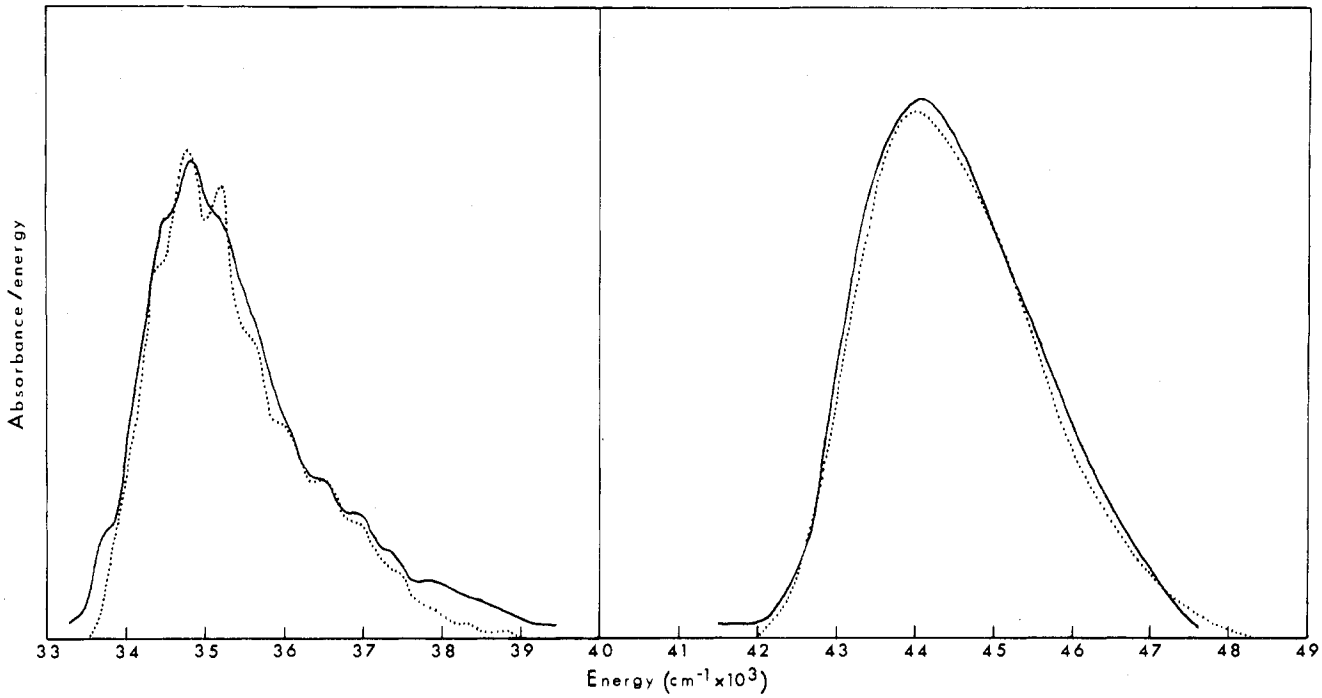

Figure 3. Comparison of the corrected experimental (full line) and generated (dotted line, reduced by a factor of 0.97 for clarity) band shapes for the intense $^1T_{1u} \leftarrow {}^1A_{1g}$ transitions in $W(CO)_6$.

lowing variables: (i) width of the Gaussian origin (b), (ii) position of the origin (c), (iii) spectral range of experimental data to be fit, (iv) background subtraction (backgrounds A and B indicated in Figure 1). Results of these checks for the first intense UV band are summarized in Table II. First, Table II (i) provides further support for a choice of 400 cm^{-1} as the width of the origin: the results obtained for ν_1 and ν_2 in the cases of b = 200 cm^{-1} and b = 800 cm^{-1} differ markedly from their experimentally observed values. Next, an estimate of the sensitivity of the parameters to the position of the origin was considered important on the basis of recent results[16] for $Co(CN)_6^{3-}$, which indicate that the position of the origin determined from a Franck–Condon fit to an overall band shape can be subject to significant error. Table II(ii) demonstrates the relative insensitivity of the S_1 parameter to this effect, and it should then be viewed as the most reliable of the parameters obtained for comparison. Furthermore, although the two transitions under consideration dominate the absorption spectra of the metal hexacarbonyls, other transitions also contribute and interfere to some extent with obtaining accurate band shapes for an isolated transition. The results contained in Table II(iii) demonstrate that the parameters are insensitive to the spectral range chosen and thus to overlap with weaker structured transitions (e.g., ligand field transitions). However, the parameters in Table II(iv) indicate that the shape of the base line does have a significant effect, particularly on the value of S_1. Thus, care was taken to be consistent in the background corrections for the two sets of transitions considered, thereby increasing the accuracy of the relative values of S_1 among the transitions.

These Franck–Condon factors can now be related to distortions (ΔQ) in the normal modes ν_1 and ν_2 by

$$S_i = \tfrac{1}{2}k_i(\Delta Q_i)^2/h\nu_i \qquad (4)$$

Values of ΔQ_i are included in Table I. From the band shape analysis of the lowest allowed transition we conclude that for both $Mo(CO)_6$ and $W(CO)_6$ there is a large distortion in the metal–carbon bond lengths and significant weakening of these bonds. Some distortion of the C–O bond also appears; however, it is not large. Although our experimental data for the second allowed transition does not furnish as detailed information, it is clear that a greater but still relatively weak distortion in carbon–oxygen bonding takes place in this excited state. We were surprised by these small C–O distortions, particularly in the case of the lower energy absorption, for transitions assigned as $M \rightarrow CO(\pi^*)$. For the $A^1\Pi \leftarrow X^1\Sigma^+$ transition of free CO, which should correspond to a similar type of one-electron excitation ($\sigma_n \rightarrow \pi^*$), a Franck–Condon factor equal to 2.2 is calculated[17] while the CO stretching frequency in $A^1\Pi$ is decreased by 655 cm^{-1} and the bond is

Table II. Sensitivity of Franck–Condon Factors and Frequencies to Controlled Variations (286-nm Band)

(i) Variation in b for $W(CO)_6$[a]

b, cm^{-1}	S_1	S_2	ν_1, cm^{-1}	ν_2, cm^{-1}
200	0.67	3.8	1110	230
400	0.33	2.7	2120	430
800	0.22	1.6	3030	740

(ii) Variation in c for $W(CO)_6$[b]

c, cm^{-1}	S_1	S_2	ν_1, cm^{-1}	ν_2, cm^{-1}
34 060	0.35	2.6	2020	410
33 920	0.33	2.8	2140	430
33 720	0.33	3.6	2170	380

(iii) Variation in Spectral Range for $W(CO)_6$[c]

range, cm^{-1}	S_1	S_2	ν_1, cm^{-1}	ν_2, cm^{-1}
34 320–39 810	0.33	2.7	2120	430
34 320–38 670	0.31	2.7	2080	420
34 000–39 000	0.32	2.8	2100	430

(iv) Variation in Background for $W(CO)_6$ and $Mo(CO)_6$[d]

bkgd[e]		S_1	S_2	ν_1, cm^{-1}	ν_2, cm^{-1}
$W(CO)_6$	A	0.32	2.8	2100	430
	B	0.24	2.7	1840	410
$Mo(CO)_6$	A	0.29	3.0	2390	420
	B	0.14	2.9	1950	380

[a] Background A; range = 34 320–39 810 cm^{-1}. [b] Background A; range = 34 320–39 810 cm^{-1}; b = 400 cm^{-1}. [c] Background A; b = 400 cm^{-1}. [d] Range = 34 000–39 000 cm^{-1}; b = 400 cm^{-1}. [e] Backgrounds A and B indicated in Figure 1.

lengthened by 0.11 Å.[18] In view of these differences, we considered the possibility that the transition at 286 nm might not be $d(t_{2g}) \rightarrow CO(\pi^*)(t_{1u})$ as is generally accepted. Klemperer's calculations for $Cr(CO)_6$ had predicted the metal-localized $d(t_{2g}) \rightarrow p(t_{1u})$ transition to lie at low energy. This excitation would be expected to result in a weakening of metal–carbon bonding. In order to further explore this possibility, a theoretical study of $Mo(CO)_6$ was begun.

B. Calculations. Calculations ranging from the extended Hückel[2] to the Hartree–Fock self-consistent field[19] (HF SCF) level have been reported for $Cr(CO)_6$. Recently the Hartree–Fock–Slater SCF (HFS SCF) or $X\alpha$ procedure has been applied to $Cr(CO)_6$.[3] In principle the HFS method involves only two approximations. The first one is the assumption that the wave function can be represented as the antisymmetrized product of one-electron wave functions, as in the HF method. One further approximation replaces the exchange-energy term in the HF equations with a local density $X\alpha$ exchange-correlation expression.[20] Simply stated, this constitutes the HFS or $X\alpha$ method. In practice there remains a problem in calculating the Coulomb energy. The integration may be facilitated by assuming spherically symmetric (muffin-tin) potentials about the atoms and a constant potential outside these spheres. Naturally this will be a poor approximation for the bonding region. It is possible to compensate for this deficiency by allowing the muffin tins to overlap (increase sphere volumes), and the latter approach constitutes the overlapping-spheres method. Another alternative is to carry out the solution to the HFS equations numerically with the discrete variational (DV) method developed by Ellis and co-workers.[9] Once again the Coulomb potential poses a problem but can be calculated by using the self-consistent charge (SCC) approximation

$$\rho_{SCC} = \sum_{inl} f_{inl} R_{nl}(r_i)^2 \qquad (5)$$

where ρ_{SCC} is the model charge density, $R_{nl}(r_i)$ are atomic radial charge densities for orbitals with quantum numbers nl located on atom i, and the f_{inl} are derived from self-consistent Mulliken orbital populations of the occupied MO's. We have chosen to adopt this latter procedure. At much greater cost ρ_{SCC} can be least-squares fitted to the molecular charge density, and Baerends and Ros have carried out such a calculation for $Cr(CO)_6$.[21] One asset of the DV method is that aside from the value of α, the exchange variable, there are no other adjustable parameters. Herein we assume $\alpha = 0.70$ to avoid empiricism. Because the DV method is a numerical method, the basis functions can be tabulated numerical basis functions (NAO's). The latter are determined from exact HFS atomic calculations. In quality this basis closely corresponds to the Clementi double-ζ basis set for atoms.[22]

We find basis set quality to be extremely important for describing the metal-localized $d \rightarrow p$ transition $3t_{2g} \rightarrow 11t_{1u}$. SCC DV $X\alpha$ computations were carried out with a minimum NAO basis set for C and O and a slightly augmented set for Mo (including 5s and 5p). A second set of calculations employed a Mo atom basis set including 5d, 6s, and 6p functions. This was done to augment the virtual orbital function space in an attempt to better describe the excited states. Addition of these lowered the virtual metallike d ($7e_g$) and p ($11t_{1u}$) orbitals by 0.71 and 2.81 eV, respectively. The expanded basis set was employed for all transition-state calculations. Table III presents results of spin-restricted transition-state calculations for the two allowed $d \rightarrow CO(\pi^*)$ charge-transfer excitations, the metal-localized $d \rightarrow p$ transition, the $CO(\sigma_n) \rightarrow Mo(5s)$ charge-transfer process, as well as the $\sigma_n \rightarrow \pi^*$ transition in free CO (σ_n = nonbonding carbon lone-pair orbital). The latter calculation tests the ability of the method to describe the lowest state of CO in which the π^* orbital is occupied. Evidently the agreement is satisfactory.

Table III. Calculated and Experimental Electronic Transition Energies for $Mo(CO)_6$ and CO

transition	type	calcd[a] energy, eV	exptl energy, eV
$3t_{2g} \rightarrow 10t_{1u}$	$d \rightarrow CO(\pi^*)$	3.95	4.32[b]
$3t_{2g} \rightarrow 2t_{2u}$	$d \rightarrow CO(\pi^*)$	4.53	5.41[b]
$3t_{2g} \rightarrow 11t_{1u}$	$d \rightarrow p$	9.75	not obsd
$9t_{1u} \rightarrow 10a_{1g}$	$CO(\sigma_n) \rightarrow s$	12.39	not obsd
$5\sigma \rightarrow 2\pi$	$\sigma_n \rightarrow \pi^*$	8.49	8.07[c]

[a] Spin-restricted transition-state calculation. [b] This work; vertical excitation. [c] G. Herzberg, "Molecular Spectra and Molecular Structure", Vol. I, Van Nostrand-Reinhold, New York, 1950. Note this reported energy is adiabatic.

Table IV. Gross Mulliken Atomic Charges for $Mo(CO)_6$ and CO

state	molecule	Mo	C	O
ground	$Mo(CO)_6$	+0.6934	+0.0028	−0.1184
$3t_{2g} \rightarrow 10t_{1u}$	$Mo(CO)_6$	+0.7336	−0.0098	−0.1125
$3t_{2g} \rightarrow 2t_{2u}$	$Mo(CO)_6$	+0.7539	−0.0133	−0.1124
ground	CO		+0.2198	−0.2198
$5\sigma \rightarrow 2\pi$	CO		+0.2087	−0.2087

The lowest allowed electronic transition in $Mo(CO)_6$ cannot result from the metal-centered $d \rightarrow p$ excitation which is predicted to lie ca. 5 eV to higher energy of the allowed $d \rightarrow CO(\pi^*)$ states. It is unlikely that the calculation be in error by as much as 5 eV. Similarly, the ligand to metal charge-transfer assignment $CO(\sigma_n) \rightarrow Mo(5s)$ is rejected on energetic grounds. Two allowed $d \rightarrow CO(\pi^*)$ transitions are predicted (Table III) 0.4 and 0.9 eV lower than the experimental values. A modest underestimation would be expected from a spin-restricted transition state which contains approximately one-fourth triplet character.[23] Because a relativistic Hamiltonian has not been used, some error will result since spin–orbit effects can be important for second-row transition-metal complexes. Since at present no relativistic calculations have been carried out for even $Cr(CO)_6$, we cannot accurately assess the importance of the relativistic correction. Complete listings of valence eigenvalues and corresponding atomic orbital populations for the $d(t_{2g}) \rightarrow CO(\pi^*)(t_{1u})$ transition state are included in the supplementary material.

Clearly we are forced to conclude that the two intense UV absorptions result from the $d(t_{2g}) \rightarrow CO(\pi^*)$ (t_{1u} and t_{2u}) transitions. Therefore, problems remain as to why the excitation to $CO(\pi^*)$ causes only a small distortion of the C–O bond and as to the relative magnitudes of this distortion for the two $^1T_{1u} \leftarrow {}^1A_{1g}$ MLCT transitions. Analysis of the corresponding transition-state charge densities provides a plausible explanation. Table IV shows the gross atomic charges for the molybdenum, carbon, and oxygen atoms in $Mo(CO)_6$ and free CO, for both the ground and the π^* excited states. From these data we conclude that when CO binds to Mo the positive charge on the carbon atom decreases dramatically, and at the same time the oxygen and molybdenum atoms become more positive. It should be remembered that a Mulliken-like analysis divides the bond charge density somewhat arbitrarily. The above changes probably are best interpreted as the effect of increased Mo–C bonding at the expense of C–O bonding. Of prime concern for our purposes are relative changes of the atomic charges in the $Mo(d) \rightarrow CO(\pi^*)$ charge-transfer states. The transitions to $CO(\pi^*)$ t_{1u} and t_{2u} do crudely correspond to charge transfer; however, the consequences are considerably different from excitation to the π^* level in free CO. In the latter example, Table IV shows that both the C and O atom charges change equally and oppositely by ca. 0.01 units of charge. For the two $Mo(d) \rightarrow CO(\pi^*)$ states in $Mo(CO)_6$ the carbon atom does pick up 0.012 and 0.016 units of charge, but the change for the oxygen

Table V. Selected Valence Orbital Decomposition into NAO Contributions for Relevant States of $Mo(CO)_6$ and CO[a]

		Mo			C		O
orbital	state	4d	5p	6p	2s	2p	2p
$3t_{2g}$	ground	0.5386				0.1959	0.2650
$3t_{2g}$	$3t_{2g} \rightarrow 10t_{1u}$	0.5662				0.1648	0.2686
$3t_{2g}$	$3t_{2g} \rightarrow 2t_{2u}$	0.5664				0.1653	0.2679
$10t_{1u}$	$3t_{2g} \rightarrow 10t_{1u}$		0.0157	0.0158	0.0513	0.7887	0.1315
$2t_{2u}$	$3t_{2g} \rightarrow 2t_{2u}$					0.8754	0.1246
2π	$5\sigma \rightarrow 2\pi$					0.9199	0.0801

[a] Only those orbitals with a contribution to the charge density >0.002 are shown. A complete listing for the $^1T_{1u}$ ($3t_{2g} \rightarrow 10t_{1u}$) state is available as supplementary material.

atom only amounts to 0.006 units in both cases. As expected, the Mo atom becomes more positive, 0.04 and 0.06 units of charge, respectively. The data also indicate that the higher energy charge-transfer state in $Mo(CO)_6$ involves greater charge reorganization, and this should lead to increased distortion of the CO moiety relative to the first charge-transfer state. The greater amount of charge reorganization in the $3t_{2g} \rightarrow 2t_{2u}$ derived state agrees with the fact that the energy of the corresponding electronic absorption band is more sensitive to solvent media than that of the $3t_{2g} \rightarrow 10t_{1u}$ transition.[2b]

At this point, it is interesting to compare the S parameters yielded by the Franck–Condon least-squares analysis of the $^1T_{1u} \leftarrow {}^1A_{1g}$ transitions with the changes in electron densities obtained from the Xα calculation on $Mo(CO)_6$. In the crude adiabatic approximation, the distorting force associated with the excited state is related to its shift in equilibrium by

$$\langle\psi_e|(\partial V/\partial Q)_0|\psi_e\rangle = +k(\Delta Q) \qquad (6)$$

where ψ_e is the excited-state electronic wave function and V is the potential, and the ground state (ψ_g) is at equilibrium ($\langle\psi_g|(\partial V/\partial Q)_0|\psi_g\rangle = 0$). Since $\langle\psi_e|(\partial V/\partial Q)_0|\psi_e\rangle$ should be roughly proportional to $\psi_e^2 - \psi_g^2$ (i.e., the change in electron density upon excitation), S should relate to the square of this quantity (eq 4). Then

$$\frac{S_1(230\text{-nm band})}{S_1(286\text{-nm band})} \simeq \frac{(\rho_{es} - \rho_{gs})^2(230\text{-nm band})}{(\rho_{es} - \rho_{gs})^2(286\text{-nm band})} \qquad (7)$$

where ρ is the integrated electron density. Using Table IV, we estimate a ratio of the FC factors of 2.3, in reasonable agreement with the ratio of 5.5 obtained from the results of the band shape analysis for $Mo(CO)_6$.

Further insight may be obtained by examining the contribution of the individual NAO's to the charge density (Table V; also see the Experimental Section). From these results we conclude that the difference between the $10t_{1u}$ and the $2t_{2u}$ orbitals reflects the differences between the two CO(π^*) charge-transfer states in $Mo(CO)_6$. Reorganization of the $3t_{2g}$ Mo(d) orbital is similar in both states (Table V). Gray[2] had earlier noted that the $2t_{2u}$ CO(π^*) orbitals were incapable of symmetry-allowed mixing with any of the valence metal orbitals. The $10t_{1u}$ orbital, however, contains a significant contribution from metal 5p and 6p functions. Even more interesting is the fact that $10t_{1u}$ mixes in substantial carbon 2s character. Klemperer's[3] calculation for $Cr(CO)_6$ also exhibited these features. Therefore, substantial Mo–C σ interaction is present in this state which agrees with the conclusion from the spectroscopic data that Mo–C bonding changes considerably in the lowest allowed transition.

When $M(CO)_6$ complexes are exposed to ultraviolet radiation, $M(CO)_5$ species and free CO are produced with high quantum efficiency.[4] Mechanistic evidence[4,24] suggests that photodissociation does not occur directly from the electronic states associated with the intense ultraviolet absorption. Rather, it is thought that fast radiationless pathways terminate in a dissociative ligand field electronic state. The presence of vibronic structure on the 286-nm absorption argues convincingly for a bound excited state. An additional structured absorption has been resolved at 242 nm in $W(CO)_6$ (Figure 1). These observations support the conclusion that direct photodissociation does not occur from these excited electronic states. Our analysis has directly probed the allowed ultraviolet absorptions in $Mo(CO)_6$ and $W(CO)_6$, and an analogous assignment seems likely for similar absorptions in $Cr(CO)_6$.

Acknowledgment. W.C.T. thanks the Research Corp. and the Northwestern University Research Committee for support of the matrix-isolation apparatus. Helpful discussions with Professors D. E. Ellis (who also provided the DVM program and instruction on its use), H. B. Gray, M. A. Ratner, and M. S. Wrighton are gratefully acknowledged. This research was supported by a Du Pont Corp. Young Faculty Grant (W.C.T.), an Alfred P. Sloan Research Fellowship (E.I.S.), the Cabot Solar Energy Fund (E.I.S.), and the Natural Sciences and Engineering Research Council of Canada (S.R.D.).

Registry No. $Mo(CO)_6$, 13939-06-5; $W(CO)_6$, 14040-11-0.

Supplementary Material Available: A complete listing of the charge-density analysis for NAO's and of one-electron energies in the $^1T_{1u}$ ($3t_{2g} \rightarrow 10t_{1u}$) state (10 pages). Ordering information is given on any current masthead page.

References and Notes

(1) (a) Northwestern University. (b) Massachusetts Institute of Technology.
(2) (a) H. B. Gray and N. A. Beach, *J. Am. Chem. Soc.*, **85**, 2922 (1963); (b) N. A. Beach and H. B. Gray, *J. Am. Chem. Soc.*, **90**, 5713 (1968).
(3) J. B. Johnson and W. G. Klemperer, *J. Am. Chem. Soc.*, **99**, 7132 (1977), and references therein.
(4) M. S. Wrighton, *Chem. Rev.*, **74**, 401 (1974).
(5) M. M. Rochkind, *Spectrochim. Acta, Part A*, **27**, 547 (1971); R. N. Perutz and J. J. Turner, *J. Chem. Soc., Faraday Trans. 2*, **69**, 452 (1973).
(6) R. N. Perutz and J. J. Turner, *J. Am. Chem. Soc.*, **97**, 4791 (1975), and references therein.
(7) D. B. Fitchen in "Physics of Color Centers", W. B. Fowler, Ed., Academic Press, New York, 1968, Chapter 5.
(8) R. B. Wilson and E. I. Solomon, *Inorg. Chem.*, **17**, 1729 (1978).
(9) A. Rosen and D. E. Ellis, *J. Chem. Phys.*, **62**, 3039 (1975); D. E. Ellis, A. Rosen, and P. F. Walch, *Int. J. Quantum Chem., Symp.*, **No. 9**, 351 (1975); P. F. Walch and D. E. Ellis, *J. Chem. Phys.*, **65**, 2387 (1976); D. D. Koelling, D. E. Ellis, and R. J. Bartlett, *ibid.*, **65**, 3331 (1976); A. Rosen and D. E. Ellis, *ibid.*, **65**, 3629 (1976); F. W. Averill and D. E. Ellis, *ibid.*, **59**, 6412 (1973).
(10) J. C. Slater, "The Self-Consistent Field for Molecules and Solids", McGraw-Hill, New York, 1974, pp 51–5.
(11) G. M. Nazarian, Ph.D. Thesis, California Institute of Technology, Pasadena, CA, 1957, cited in ref 1.
(12) K. N. Rao, *Astrophys. J.*, **110**, 304 (1949).
(13) M. D. Sturge, *Solid State Phys.*, **20**, 91 (1967).
(14) L. H. Jones, *Spectrochim. Acta*, **19**, 329 (1963).
(15) R. B. Wilson and E. I. Solomon, submitted for publication in *Inorg. Chem.*
(16) V. M. Miskowski, H. B. Gray, R. B. Wilson, and E. I. Solomon, *Inorg. Chem.*, **18**, 1410 (1979).
(17) This value was calculated from overlap integrals for excited-state vibrational quantum numbers ranging from 0 to 7. The overlap integrals were obtained from Professor Robert W. Field (private communication).
(18) G. Herzberg, "Molecular Spectra and Molecular Structure", Vol. I, Van Nostrand-Reinhold, New York, 1950, pp 154, 522.
(19) I. H. Hillier and V. R. Saunders, *Mol. Phys.*, **22**, 1025 (1971).
(20) Reference 10, pp 21–6.
(21) E. J. Baerends and P. Ros, *Mol. Phys.*, **30**, 1735 (1975).
(22) K. Schwarz and J. W. D. Connolly, *J. Chem. Phys.*, **55**, 4710 (1971).
(23) P. S. Bagus and B. I. Bennett, *Int. J. Quantum Chem.*, **9**, 143 (1975).
(24) J. Nasielski and A. Colas, *Inorg. Chem.*, **17**, 237 (1978).